Journal of
Nanoscience and Nanotechnology
Vol. 13, 4975–4980, 2013

Nano Cu Metal Doped on TiO_2–SiO_2 Nanoparticle Catalysts in Photocatalytic Degradation of Direct Blue Dye

R. M. Mohamed[1, 2], I. A. Mkhalid[1], S. A. Al-Thabaiti[1], and Mohamed Mokhtar[1, *]

[1] *Faculty of Science, Chemistry Department, King Abdulaziz University, P.O. Box: 80203 Jeddah 21589, Saudi Arabia*
[2] *Advanced Materials Department, Central Metallurgical R&D Institute, CMRDI, P.O. Box 87 Helwan, Cairo, 11421, Egypt*

The photo-assisted deposition (PAD) and impregnation (Img) synthesis of nano-sized Cu metal on TiO_2–SiO_2 are reported. The prepared catalysts were characterized by different techniques such as XRD, EXAFS, TEM and nitrogen adsorption analysis. Photocatalytic reactivity using Cu–TiO_2–SiO_2 catalysts under visible-light condition on the oxidation of direct blue dye with O_2 reaction was evaluated. The results have shown notable photocatalytic activity of PAD-Cu/TiO_2–SiO_2 which was 1.6 and 10 times higher than that of Img-Cu/TiO_2–SiO_2 and TiO_2–SiO_2, respectively.

Keywords: Visible Photocatalyst, Cu-Doped Titania-Silica, Direct Blue Dye.

RESEARCH ARTICLE

1. INTRODUCTION

TiO_2 photocatalysis is a much appreciated in recent years for environmental improvement such as the photodegradation and complete mineralization of organic pollutants.[1, 2] TiO_2 nanoparticles have large specific surface areas and high catalytic performance in which reactions take place on the TiO_2 surface. However, their effective commercial applications are hindered by three serious disadvantages. Firstly, agglomerations of ultrafine powders into larger particles result in an adverse effect on catalyst performance. Secondly, the separation and recovery of TiO_2 powders from wastewater are complicated.[3, 4] Thirdly, the requirements of ultraviolet (UV) radiation for TiO_2 photocatalysis performance whose energy exceeds the band gap of 3.2 eV ($\lambda - 380$ nm) of the anatase crystalline phase, which in turn led utilization only a very small fraction of sunlight.

More recently, TiO_2 has attracted the attention of scientists in the catalysis field, due to its effective utilization of visible light to degrade organic pollutants. A considerable effort has been devoted to develop supported titania catalysts offering high active surface area, while at the same time having easier separation and removal from wastewater.[5, 6] New synthesis methods of titania-silica mixed oxides are needed for overcoming the present disadvantages of pure titania powders. One of the ways is the use of charge-transfer catalysts, which can improve the efficiency of TiO_2. This type can be obtained by the preparation of TiO_2–SiO_2 catalyst with the electron transfer across the solid–solid TiO_2–SiO_2 interface. For that reasons, in a previous study it was reported that the TiO_2–SiO_2 catalyst is three times more photoactive than TiO_2 alone.[7–9] Another possibility is to modify TiO_2 by surface deposition of noble metals to shift the process of photodegradation of organic pollutants into the visible-light region.[10–13]

Recently, there is much interest in a new nano-sized catalyst such as Pd, Pt, and Au as potentially advanced materials possessing unique electronic, optic and magnetic properties as well as catalytic functions.[14–16] One of the most important factors for controlling catalytic activity of these metal catalysts is the particle size. The development of convenient and useful method to prepare the nano-sized metal loaded on support with controlled particle size and size distribution is an essential task to design a highly active metal catalyst.

Under UV-light irradiation, these single-site photocatalysts generate charge transfer excited state which can show the highly active and selective photocatalytic performances. In previous studies,[18–27] the main focus has been made only on the photocatalytic reactivity but the applications of single-site photocatalyst for the synthesis of conventional catalysts such as nano-sized metal catalyst have not been yet reported. It can be expected that the metal

*Author to whom correspondence should be addressed.

precursor species can be easily deposited on the excited state of single-site photocatalyst to form well-controlled sized metal particles from the mixture of single-site photocatalyst in the aqueous solution with metal precursor.

In the present study, Cu/TiO_2–SiO_2 was prepared by the application of a photo-assisted deposition (PAD) and impregnation methods. We focus on the photocatalytic reactivity of Cu/TiO_2–SiO_2 under visible-light for the oxidation of direct blue dye.

2. EXPERIMENTAL DETAILS

2.1. Materials

All chemicals used in this study were used as received without any further purification. Titania–silica mixed oxides were prepared by the hydrolysis of ammonia water (NH_3, 25%). Titanium tetrabutoxide (TBOT, $\geq$98%)/and tetraethyl orthosilicate (TEOS, $\geq$98%) were selected as the source of titania and silica, respectively. Here, we give a typical procedure for the preparation of titania–silica mixed oxide containing 16.6 mol% of silica. Firstly, 17.0 ml TBOT was mixed with 5.1 ml acetylacetone and 10.0 ml anhydrous ethyl alcohol. Secondly, 2.25 ml TEOS was mixed with the solution containing 10.8 ml bidistilled water, 23.9 ml ammonia water and 20.0 ml anhydrous ethyl alcohol under stirring. At the final step, Ti and Si sols were added simultaneously and slowly into the beaker containing 10.0 ml anhydrous ethyl alcohol under stirring. After the end of the above operations, the samples were aged in the beaker covered by a plastic film for 72 h. Finally, the samples obtained were evaporated and dried, followed by calcination at 550 °C for 5 h in air.

On the other side, the Cu loaded on TiO_2–SiO_2 (PAD-Cu/TiO_2–SiO_2, 3 wt% as Cu metal) was prepared using the PAD method: Cu metal was deposited on TiO_2–SiO_2 from aqueous solution of Cupper nitrate under UV-light irradiation. The Cu loaded on TiO_2–SiO_2 (img-Cu/TiO_2–SiO_2, 3 wt% as Cu metal) was prepared using impregnation method: the Cu metal was deposited by a simple impregnation of TiO_2–SiO_2 in the absence of light with aqueous solution of Cupper nitrate. The samples were dried at 378 K and reduced by H_2 (20 ml min^{-1}) at 473 K for 2 h.

2.2. Characterization Techniques

The structure of the catalyst was examined by X-ray diffraction (XRD) on a Rigaku X-ray diffractometer system equipped with as RINT 2000 wide angle Goniometer using Cu Kα radiation and a power of 40 kV $\times$ 30 mA. The intensity data were collected at 25 °C over a 2θ range of 20–80°. The UV-vis diffuse reflectance absorption spectra were recorded with a Shimadzu UV-2450 at 295 K. The X-ray absorption fine structure (XAFS) analysis, X-ray absorption near edge structure (XANES) and extended X-ray absorption fine structure (EXAFS), were performed at BL-7C facility[28] of the Photon Factory at the National Laboratory for High-Energy Physics, Tsukuba, Tokyo, Japan. A Si(111) double crystal was used to monochromatize the X-rays from the 2.5 GeV electron storage ring. The K-edge XAFS spectra of Cu was measured in the fluorescence mode at 298 K. The normalized spectra were obtained by a procedure described in a previous study[29] and Fourier transformed was performed on k^3-weighted EXAFS oscillations in the range of 1–10 $Å^{-1}$. N_2-adsorCuion measurement was carried out at 77 K using Nova 2000 series, Chromatech. Prior to analysis, the samples were outgased at 250 °C for 4 h. The morphology and particle size of the prepared samples were examined via a transmission electron microscope (Hitachi H-9500 operated at 300 kv).

2.3. Photocatalytic Reaction

The photocatalytic reactions were carried out in a quartz cell (28 mm in diameter and 200 mm in height). The photocatalyst (50 mg) was located in a quartz cell with an aqueous solution of direct blue dye (100 ppm, 25 ml). Prior to exposure to a visible light, the suspension was stirred in a flow of O_2 for 1 h under dark atmosphere. The sample was then irradiated with a visible light, which was generated by a 100 W high-pressure mercury lamp and an appropriate cut off filter was placed in the front of the reactor to remove the part of UV radiation. The catalysts and solution were separated by filtration and then the resulting solution was analyzed by Shimadzu UV-2450.

3. RESULTS AND DISCUSSION

3.1. Evaluation and Characterization of Synthesized Material

3.1.1. XRD Analysis

XRD patterns of each parent TiO_2–SiO_2 and Cu-doped TiO_2–SiO_2 nanoparticles prepared by Impregnation method, and PAD, methods are compared in Figure 1. The structural characteristic of TiO_2–SiO_2 and all Cu-doped TiO_2–SiO_2, are mainly composed of anatase phase containing a group of lines at 2θ values of 25.2, 37.5, 47.7, 53.3, 54.7 and 62° [PDF 71-1169], which indicated that, titania anatase phase structure was remained after the application of the photo-assisted deposition (PAD) and impregnation methods. However, no diffraction peaks of copper in the patterns of Cu-doped samples were observed. This is probably attributed to the low Cu doping content (*ca.* 3%). Moreover, the data may imply that, the copper is well dispersed within the TiO_2–SiO_2 phase.

3.1.2. UV-Vis Spectroscopy

Figure 2 depicts the diffuse reflectance UV-vis absorption spectra of TiO_2–SiO_2, PAD-Cu/TiO_2–SiO_2 and

RESEARCH ARTICLE

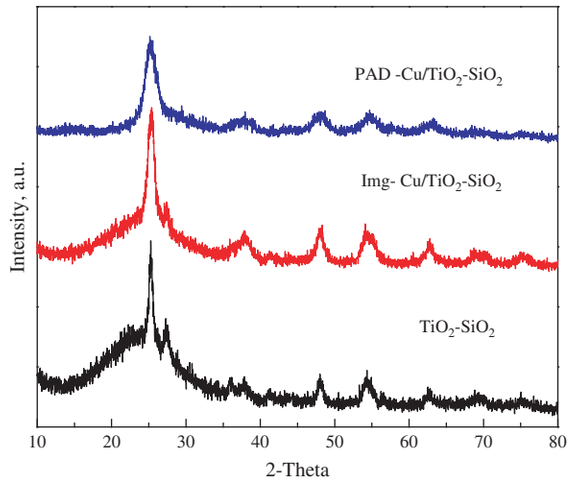

Fig. 1. XRD patterns of the TiO_2–SiO_2, PAD-Cu/TiO_2–SiO_2 and img-Cu/TiO_2–SiO_2.

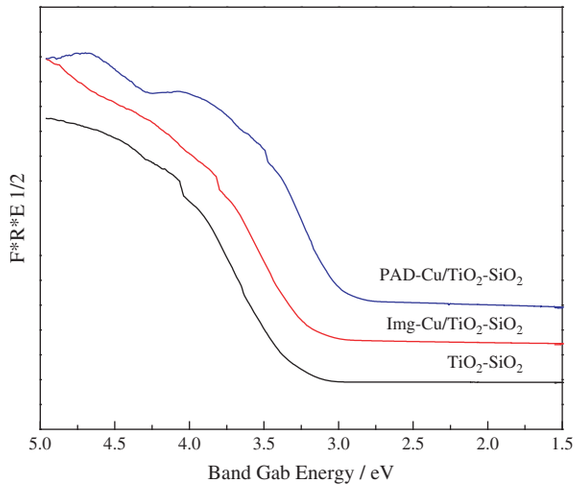

Fig. 3. Band-gap calculated from the DR-UV-vis spectra.

imp-Cu/TiO_2–SiO_2. The Kubelka–Munk function, $F(R)$, can be considered to be proportional to the absorption of radiation.[29] On this basis, the value of E_g, the band gap of the semiconductor, can be derived from the spectra by plotting $(F(R) \cdot h\nu)^{1/2}$ against $h\nu$ as shown in Figure 3.[30] The band-gap values usually reported for pure anatase and rutile phases are 3.2 and 3.03 eV, respectively.[31] However, these values are influenced by the synthesis method, and also affected by the existence of impurities doping the crystalline network and also the average crystal size of the semiconductor. In a previous study, different methods for calculating the E_g from the UV-vis reflectance spectra are used. For example, some authors calculate the E_g values by a direct extrapolation of the $F(R)$ spectrum whereas others report the wavelength corresponding to the maximum absorption.[32] As a consequence, quite different E_g values for rutile and anatase samples are found in the literature. For instance, for anatase-based materials the threshold wavelength values of 370 nm,[33] 380 nm,[34] 387 nm,[35] 393 nm[36] and 403 nm has been reported[37] corresponding to a band gap range from 3.08 to 3.35 eV have been reported. In the case of rutile-based materials, an absorption wavelength as high as 437.4 nm (E_g = 2.84 eV).[37] In the present study (Fig. 3), the band gap values calculated for TiO_2–SiO_2, PAD-Cu/TiO_2–SiO_2 and Img-Cu/TiO_2–SiO_2 are 3.19, 2.83 and 2.53 eV, respectively. Therefore, the study of UV-vis radiation absorption constitutes an important tool for the evaluation of the changes produced in the semiconductor materials by different treatments.

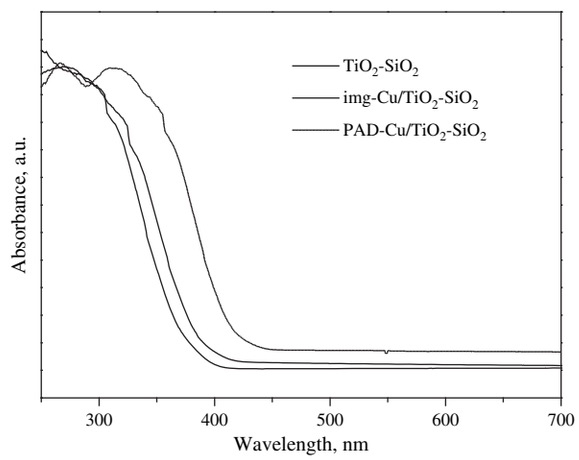

Fig. 2. Diffuse reflectance UV-vis absorption spectra of TiO_2–SiO_2, PAD-Cu/TiO_2–SiO_2 and img-Cu/TiO_2–SiO_2.

3.1.3. Specific Surface Area Trends

The surface parameters of surface area and the data calculated from the *t*-plot. The N_2 adsorption isotherms (not shown here) for the parent and the Cu-TiO_2–SiO_2 are typical of mesoporous solids (type IV), however, an increase in the adsorption capacity of the TiO_2–SiO_2 was observed after introducing Cu ions. The surface area changed from 720 (parent TiO_2–SiO_2) to 640 and 690 m^2/g in case of img-Cu/TiO_2–SiO_2 and PAD-Cu/ TiO_2–SiO_2 respectively. The surface texture data are correlated with the catalytic activity as will be mentioned later on.

3.1.4. EXAFS Analysis

The Fourier transforms of Cu LIII-edge EXAFS spectra of the Cu-loaded catalysts are shown in Figure 4. The presence of the peak assigned to the Cu—Cu bond of Cu metal at around 2.93 Å indicates the formation of nano-sized Cu metal.[38] The intensity of the Cu—Cu peak of the PAD-Cu/TiO_2–SiO_2 catalyst is smaller than the img-Cu/TiO_2–SiO_2 catalyst. These findings suggest that the size of Cu metal particles depends on the preparation

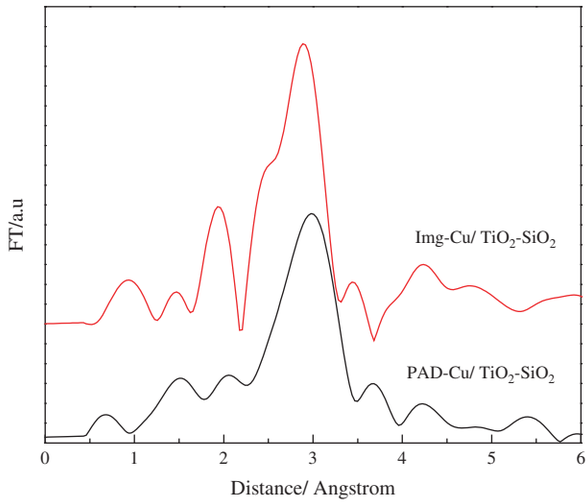

Fig. 4. Fourier transforms of the Cu LIII-edge EXAFS spectra for img-Cu/TiO_2–SiO_2 and PAD-Cu/TiO_2–SiO_2.

method. Cu metal particles formed on the photo-deposited catalyst (PAD-Cu/TiO_2–SiO_2) show smaller particle size than that of the impregnated catalyst (img-Cu/TiO_2–SiO_2). In addition to that, we can control the size of the Cu particles by varying content of Ti oxide, light intensity and light wavelength.

3.1.5. TEM Observation

The TEM images of PAD-Cu/TiO_2–SiO_2 and imp-Cu/TiO_2–SiO_2 catalysts are shown in Figure 5. The particle size distribution obtained from the analysis of TEM images are also shown in Figure 6. In agreement with the results of EXAFS measurement, the nano-sized Cu metal with a mean diameter (d) of ca. 4 nm having a narrow size distribution was found on the PAD-Cu/TiO_2–SiO_2 catalyst, whereas the aggregated Cu metal with various sizes are observed on img-Cu/TiO_2–SiO_2 catalyst ($d = 14$ nm).

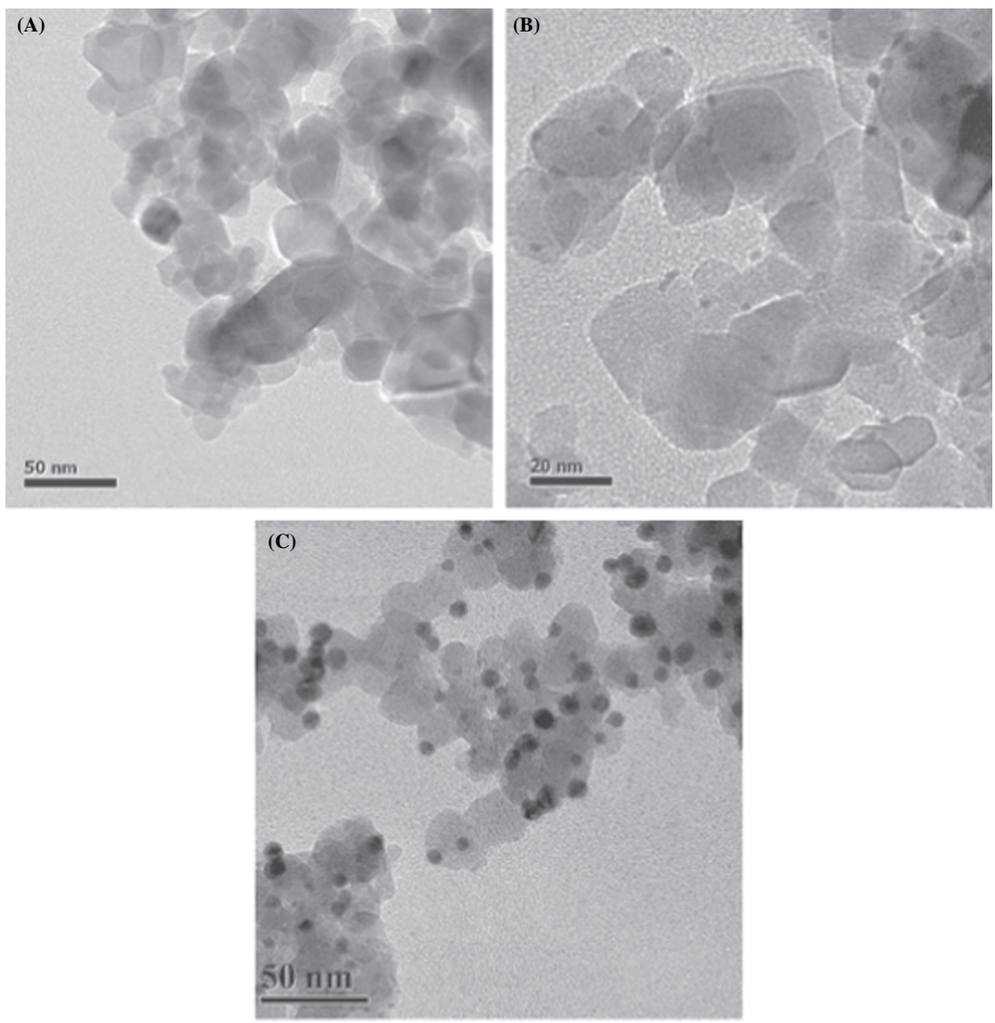

Fig. 5. The TEM images of the TiO_2–SiO_2 (A), PAD-Cu-TiO_2–SiO_2 (B) and img-Cu-TiO_2–SiO_2 (C) catalyst after H_2 treatment at 200 °C.

RESEARCH ARTICLE

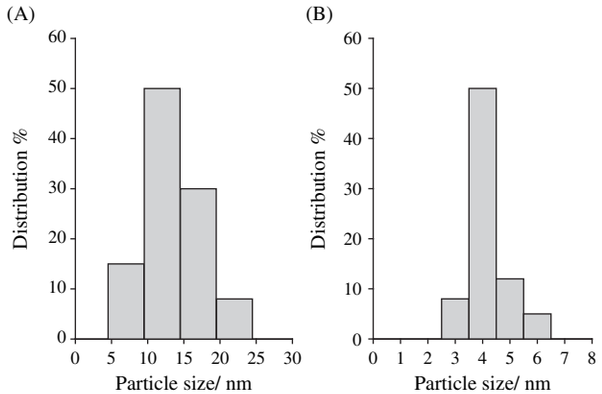

Fig. 6. Size distribution diagrams of Cu metal obtained from the TEM images of the img-Cu/TiO_2–SiO_2 (A) and PAD-Cu-TiO_2–SiO_2 (B) catalyst after H_2 treatment at 200 °C.

3.2. Photocatalytic Degradation of Direct Blue Dye

The photocatalytic degradation of direct blue dye is used as a probe reaction to test the catalytic activity of the prepared nanoparticles. The effect of TiO_2–SiO_2, img-Cu/TiO_2–SiO_2 and PAD-Cu/TiO_2–SiO_2 on photocatalytic oxidation of direct blue dye after 60 min. at room temperature using (100 ppm, 25 ml) of the direct blue dye and 50 mg catalyst are shown in Figure 7. The data demonstrates that the photocatalytic activities of the PAD-Cu/TiO_2–SiO_2 are higher than that of img-Cu/TiO_2–SiO_2 and parent TiO_2–SiO_2. Considering that, the pure Cu oxides don't have photocatalytic oxidation properties, such variation in activity must be due to the differences in interaction between Cu and TiO_2–SiO_2 that led to several modifications in physical properties such as band gap, particle size and surface texture. Also, we can observe that, the catalytic activity of TiO_2–SiO_2 generally increased with the addition of Cu promoters. A maximum activity was obtained in case of PAD-Cu/TiO_2–SiO_2. It is clear that, the photocatalytic activity was a maximum in the case of PAD-Cu-TiO_2–SiO_2 in which the surface area was the biggest but band gap was the lowest value.

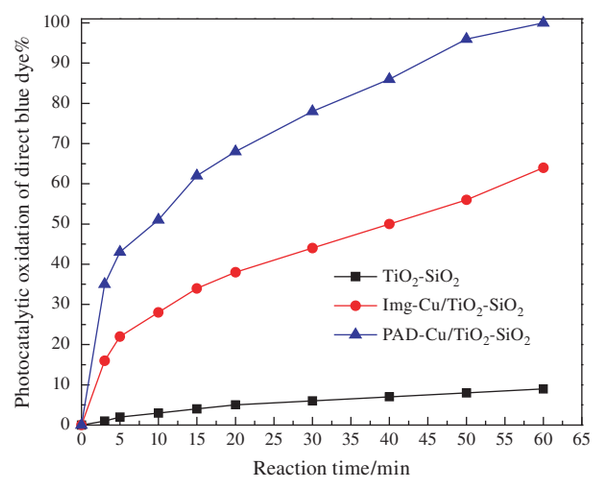

Fig. 7. Photocatalytic degradation of direct blue dye, % for TiO_2–SiO_2, img-Cu/TiO_2–SiO_2 and PAD-Cu/TiO_2–SiO_2.

It is believed that, the lack of electron scavengers (surface Ti^{4+}) and hole traps (surface hydroxyl groups) is responsible for the rapid recombination rate of e^-/h^+, which leads to lower photocatalytic activity. The results show that the photocatalytic activities of the Cu doped TiO_2–SiO_2 nanoparticles increased with decreasing the band gap. This is due to the low energy to exit electron from valance band to conduction band. Also, the PAD-Cu/TiO_2–SiO_2 has the best photoactivity, since it has the lowest band gap and particle size and the highest surface area and pore volume.

4. CONCLUSIONS

It can be concluded that the nano-sized particles of Cu/TiO_2–SiO_2 can be prepared via two methods: photo-assisted deposition (PAD) and the conventional impregnation method. The characterization of such prepared catalysts by N_2 adsorption, XRD, UV-vis and XAFS techniques reveals the following remarks:

(1) The nano-sized Cu metal with a mean diameter (d) of ca. 4 nm having a narrow size distribution was found on the PAD-Cu/TiO_2–SiO_2 catalyst, whereas the aggregated Cu metal with various sizes are observed on img-Cu/TiO_2–SiO_2 catalyst ($d = 14$ nm).

(2) The calculated values of band gap for TiO_2–SiO_2, img-Cu/TiO_2–SiO_2 and PAD-Cu/TiO_2–SiO_2. are 3.19, 2.83 and 2.53, respectively.

(3) The N_2 adsorption isotherms for the parent and the Cu-TiO_2–SiO_2 are typical of mesoporous solids, the surface area changed from 720 to 690 and 640 m^2/g in case of TiO_2–SiO_2, PAD-Cu/TiO_2–SiO_2 and img-Cu/TiO_2–SiO_2 respectively.

(4) The intensity of the Cu—Cu peak of the PAD-Cu-TiO_2–SiO_2 catalyst is smaller than the img-Cu/TiO_2–SiO_2 catalyst. These findings suggest that the size of Cu metal particles depends on the preparation method. Cu metal particles formed on the photo-deposited catalyst (PAD-Cu/TiO_2–SiO_2) shows smaller particle sizes than that obtained from the impregnated catalyst (img-Cu/TiO_2–SiO_2).

In summary, using the PAD method and TiO_2–SiO_2, nano sized Cu metal particles with a well-controlled size and a well dispersed state can be deposited on tetrahedrally coordinated Ti-oxide of the support. The direct interaction between nano-sized Cu metal and the photo-excited tetrahedrally coordinated Ti-oxide realized by the PAD method under UV-light irradiation have the possibility to design the unique and active nano-sized metal catalyst.

RESEARCH ARTICLE

References and Notes

1. A. Linsebigler, G. Lu, and J. T. Yates, *Chem. Rev.* 735, 95 (**1995**).
2. A. Fujishima, N. T. Rao, and D. A. Rryk, *J. Photochem. Photobiol. C Revs.* 1, 1 (**2000**).
3. J. B. Christophe, A. Francine, C. Pascal, J. Marie, and L. Frank, *Ceram J. Am. Soc.* 80, 3157 (**1997**).
4. Y. Zhu, L. Zhang, W. Yao, and L. Cao, *Appl. Surf. Sci.* 158, 32 (**2000**).
5. P. T. Tanev, M. Chibwe, and T. J. Pinnavaia, *Nature* 368, 321 (**1994**).
6. J. V. Walker, M. Morey, H. Carlsson, A. Davidson, G. D. Stucky, and A. J. Butler, *Chem. J. Am. Soc.* 119, 6921 (**1997**).
7. A. J. Anderson and A. J. Bard, *Phys J. Chem.* 99, 9882 (**1995**).
8. S. A. Ruetten and J. K. Thomas, *Photochem. Photobiol. Sci.* 2, 1018 (**2003**).
9. H. Chun, Y. Wang, and H. Tang, *Appl. Catal. B Environ.* 30, 277 (**2001**).
10. C. Y. Wang, C. Y. Liu, and X. Zheng, *Colloids Surf. A Physicochem. Eng. Asp.* 131, 271 (**1998**).
11. J. C. Yang, Y. C. Kim, and Y. G. Shul, *Appl. Surf. Sci.* 121, 525 (**1997**).
12. H. Kisch, L. Zang, C. Lange, W. F. Maier, C. Antonius, and D. Meissner, *Angew. Chem., Int. Ed.* 37, 3034 (**1998**).
13. F. B. Li and X. Z. Li, *Appl. Catal. A: Gen.* 228, 15 (**2002**).
14. K. Mori, T. Hara, T. Mizugaki, K. Ebitani, and K. Kaneda, *J. Am. Chem. Soc.* 126, 10657 (**2004**).
15. A. Fukuoka, H. Araki, J. Kimura, Y. Sakamoto, T. Higuchi, N. Sugimoto, S. Inagaki, and M. Ichikawa, *J. Mater. Chem.* 14, 752 (**2004**).
16. F. Boccuzzi, A. Chiorino, M. Manzoli, P. Lu, T. Akita, S. Ichikawa, and M. Haruta, *J. Catal.* 202, 256 (**2002**).
17. M. Anpo and J. M. Thomas, *Chem. Commun.* 3273 (**2006**).
18. H. Yamashita and M. Anpo, *Curr. Opin. Solid State Mater. Sci.* 7, 471 (**2004**).
19. M. Anpo and M. Che, *Adv. Catal.* 44, 119 (**1999**).
20. H. Yamashita, K. Ikeue, T. Takewaki, and M. Anpo, *Topics in Catal.* 18, 95 (**2002**).
21. K. Ikeue, H. Yamashita, T. Takewaki, and M. Anpo, *J. Phys. Chem. B.* 201, 8350 (**2001**).
22. M. Anpo, H. Yamashita, Y. Ichihashi, Y. Fujii, and M. Honda, *J. Phys. Chem. B.* 101, 2632 (**1997**).
23. M. Anpo, H. Yamashita, Y. Ichihashi, M. Anpo, M. Hasimoto, C. Louis, and M. Che, *J. Phys. Chem.* 100, 16041 (**1996**).
24. H. Yamashita, K. Yoshizawa, M. Ariyuki, S. Higashimoto, M. Che, and M. Anpo, *Chem. Commun.* 435 (**2001**).
25. C. Murata, H. Yoshida, and T. Hattori. *Chem. Commun.* 2412 (**2001**).
26. F. Amano, T. Yamaguchi, and T. Tanaka, *J. Phys. Chem. B.* 109, 281 (**2006**).
27. N. Ichikuni, H. Murayama, K. K. Bando, S. Shimazu, and T. Uematsu, *Anal. Sci.* 17, 1193 (**2001**).
28. N. Masaharu and K. Atsushi, *J. Synchrotron Rad.* 6, 182 (**1999**).
29. C. Anderson and A. J. Bard, *J. Phys. Chem. B.* 101, 2611 (**1997**).
30. G. Lassaleta, A. Fernaandez, J. P. Espinoos, and A. R. Gonzaolez-Elipe, *J. Phys. Chem.* 99, 1848 (**1995**).
31. M. Schiavello (Ed.), Heterogeneous Photocatalysis, Wiley, Chichester (**1997**).
32. R. J. Davis and Z. Liu, *Chem. Mater.* 9, 2311 (**1997**).
33. D. F. Ollis, *Catal. Technol.* 2, 149 (**1998**).
34. K. Kosuge and S. Singh, *J. Phys. Chem. B.* 18, 3563 (**1999**).
35. A. A. Belhekar, S. V. Awate, and R. Anand, *Catal. Commun.* 3, 453 (**2002**).
36. B. J. Aronson, C. F. Blanford, and A. Stein, *Chem. Mater.* 9, 2842 (**1997**).
37. S. Cheng, S. Tsai, and Y. Lee, *Catal. Today* 26, 87 (**1995**).
38. T. E. Alcacio, D. Hesterberg, J. W. Chou, J. D. Martin, S. Beauchemin, and D. E. Sayers, *Geochimica et Cosmochimica Acta* 65, 1355 (**2001**).

Received: 11 November 2012. Accepted: 16 February 2103.

RESEARCH ARTICLE